



Molecular Aspects of Adipose-Derived Stromal Cell Senescence in a Long-Term Culture: A Potential Role of Inflammatory Pathways

Cell Transplantation
Volume 29: 1–13
© The Author(s) 2020
Article reuse guidelines:
sagepub.com/journals-permissions
DOI: 10.1177/0963689720917341
journals.sagepub.com/home/ccl


Marta Pokrywczynska^{1,*}, Małgorzata Maj^{1,2,*}, Tomasz Kloskowski¹ ,
Monika Buhl¹, Daria Balcerzyk¹, Arkadiusz Jundziłł^{1,3},
Kamil Szeliski¹, Marta Rasmus¹, and Tomasz Drewa^{1,2}

Abstract

Long-term culture of mesenchymal stromal/stem cells *in vitro* leads to their senescence. It is very important to define the maximal passage to which the mesenchymal stromal/stem cells maintain their regenerative properties and can be used for cellular therapies and construction of neo-organs for clinical application. Adipose-derived stromal/stem cells were isolated from porcine adipose tissue. Immunophenotype, population doubling time, viability using bromodeoxyuridine assay, MTT assay, clonogenicity, β -galactosidase activity, specific senescence-associated gene expression, apoptosis, and cell cycle of adipose-derived mesenchymal stromal/stem cells (AD-MSCs) were analyzed. All analyses were performed through 12 passages (P). Decreasing viability and proliferative potential of AD-MSCs with subsequent passages together with prolonged population doubling time were observed. Expression of β -galactosidase gradually increased after P6. Differentiation potential of AD-MSCs into adipogenic, chondrogenic, and osteogenic lineages decreased at the end of culture (P10). No changes in the cell cycle, the number of apoptotic cells and expression of specific AD-MSC markers during the long-term culture were revealed. Molecular analysis showed increased expression of genes involved in activation of inflammatory response. AD-MSCs can be cultured for *in vivo* applications without loss of their properties up to P6.

Keywords

adipose-derived stromal/stem cell, aging, senescence, long-term culture, gene expression

Introduction

Multipotent mesenchymal stromal/stem cells isolated from adipose tissue in last years have become the leading type of cells used for tissue engineering application¹. Advantage of this cell source compared to other sources like bone marrow is greater availability and minimally invasive adipose tissue harvesting technique². Isolated cells have highly proliferative and multidifferentiative potential³. Properties of AD-MSCs (adipose-derived mesenchymal stromal/stem cells) were well established, thanks to increasing use of this cell type in large number of studies⁴. Analysis of immunophenotype, proliferation and differentiation potential, clonogenicity, and other tests are standard procedures performed to confirm multipotent properties of isolated cells. These assessments were performed in most studies at early stages of culture, usually after three or four passages. Data about AD-MSC characteristics during long-term culture are

¹ Department of Regenerative Medicine, Cell and Tissue Bank, Chair of Urology, Collegium Medicum, Nicolaus Copernicus University, Bydgoszcz, Poland

² Department of Tissue Engineering, Department of Regenerative Medicine, Cell and Tissue Bank, Chair of Urology, Collegium Medicum, Nicolaus Copernicus University, Bydgoszcz, Poland

³ Department of Plastic, Reconstructive and Aesthetic Surgery, Collegium Medicum, Nicolaus Copernicus University, Bydgoszcz, Poland

* Both the authors contributed equally to this article

Submitted: September 3, 2019. Revised: February 25, 2020. Accepted: March 13, 2020.

Corresponding Author:

Marta Pokrywczynska, Department of Regenerative Medicine, Cell and Tissue Bank, Nicolaus Copernicus University, Collegium Medicum, M. Skłodowskiej-Curie 9, 85-094 Bydgoszcz, Poland.
Email: marta.pokrywczynska@interia.pl



Creative Commons Non Commercial CC BY-NC: This article is distributed under the terms of the Creative Commons Attribution-NonCommercial 4.0 License (<https://creativecommons.org/licenses/by-nc/4.0/>) which permits non-commercial use, reproduction and distribution of the work without further permission provided the original work is attributed as specified on the SAGE and Open Access pages (<https://us.sagepub.com/en-us/nam/open-access-at-sage>).

missing^{5,6}. Construction of large organs like neo-bladder or neo-conduit using tissue engineering techniques require large number of cells. It was indicated that cells seeded in large density ($50 \times 10^6/\text{cm}^3$, $10 \times 10^6/\text{cm}^2$) promoted urinary bladder regeneration more effectively protecting from scar formation^{7,8}. Higher cell density increases process of regeneration by extending time of viable cells secreting growth factors, which enhance proper well-organized cell layers reconstruction⁸. Such high cell number can be difficult to achieve from early passages especially in cases when the amount of adipose tissue is limited. That is why it is very important to show how long AD-MSCs retain their regenerative properties and determine the maximum passage after which AD-MSCs can be used for clinical applications without signs of senescence.

The aim of this study was to analyze the regenerative properties of AD-MSCs isolated from porcine adipose tissue in long-term culture. Immunophenotype, proliferation and differentiation potential, clonogenicity, senescence markers, cell cycle, and apoptosis were analyzed in order to determine the maximum cultivation time after which AD-MSCs maintain their regenerative properties and can be used for in vivo studies.

Materials and Methods

Animals

The study was performed with the permission of the Local Ethics Committee (no. 30/2013). Ten female domestic pigs included in this study weighed between 30 and 40 kg (age 10 to 12 wk). Adipose tissue was harvested from subcutaneous tissue of the abdominal wall. Adipose tissue immediately after resection was transferred to containers with Dulbecco's Modified Eagle's Medium/ Ham's F12 (GE Healthcare Life Science, Logan, UT, USA) supplemented with antibiotics: penicillin (100 U/ml, GE Healthcare Life Science), streptomycin (100 µg/ml, GE Healthcare Life Science), amphotericin B (5 µg/ml, BD Bioscience, Franklin Lakes, NJ, USA) and transported to the laboratory.

Isolation and Culture of Porcine Adipose-derived Stromal/Stem Cells

The adipose tissue was washed twice with deionized water and twice with phosphate-buffered saline (PBS; Pan-Biotech, Aidenbach, Germany) supplemented with antibiotics: 100 U/ml penicillin, 100 µg/ml streptomycin, and 5 µg/ml amphotericin B. The adipose tissue was purified by blood vessel resection. Next, 32 g of adipose tissue from each animal was washed twice with PBS supplemented with antibiotics, cut to small pieces and equally divided into four tubes. Samples were digested in the mixture of collagenase P (1 mg/ml, Sigma-Aldrich, Steinheim, Germany), calcium chloride (5 mM, Sigma-Aldrich), Hank's Balanced Salt Solution (Pan-Biotech), and HEPES Buffer (PAA, Pasching,

Austria) at a concentration of 1 ml enzyme/1 g of tissue in a shaking water bath for 60 min at 37°C. After digestion, the collagenase P was neutralized by adding an equal volume of DMEM/Ham's F12 supplemented with 10% fetal bovine serum (FBS; Pan-Biotech), 100 U/ml penicillin, 100 µg/ml streptomycin, and 5 µg/ml amphotericin B. Next, the samples were filtered through 100 µm cell strainer (BD Bioscience) and centrifuged at $1,200 \times g$ for 5 min. After centrifugation the supernatant was removed using Pasteur pipette (BD Bioscience) and the pellet was resuspended in DMEM/F12 supplemented with 10% FBS, 10 ng/ml basic fibroblast growth factor (Thermo Fisher Scientific, Waltham, MA, USA), 100 U/ml penicillin, 100 µg/ml streptomycin, and 5 µg/ml amphotericin B. Number of cells was determined by trypan blue exclusion. Isolated cells were seeded at a density of 2×10^4 cells/cm². Cells were cultured at 37°C in 5% CO₂ and 95% humidity. Growth medium was changed every 2 d. Cell morphology and growth were evaluated under inverted light microscope (Leica, Wetzlar, Germany). Cells were cultured until the 12th passage.

Cell Surface Markers Expression

Phenotypic analysis of cell surface markers, including CD29, CD44, CD90, CD11b, CD31, and CD45, was performed every second passage. Appropriate isotype controls were used to determine the levels of background fluorescence. For each marker, approximately 0.5×10^6 cells were used for analysis. Cells were washed twice in PBS, centrifuged for 5 min at $700 \times g$ and suspended in 200 µl of Staining Buffer (BD Bioscience) containing 2% FBS and 0.09% sodium azide. Appropriate amounts of specific antibodies were pipetted to each tube (Table 1). Cells were then incubated for 30 min in the dark at 4°C. After incubation cells were washed twice with Staining Buffer and analyzed with the use of FACSCanto II flow cytometer (BD Bioscience).

Population Doubling Time (PDT)

Growth kinetics in long-term culture was monitored by counting cell number in subsequent passages with the use of hemocytometer and trypan blue. PDT was calculated according to the formula $PDT = T \ln 2 / \ln(N_2 - N_1)$, where T is the incubation time, N_1 is the cell number at the beginning of the incubation, and N_2 is the cell number at the end of the incubation.

Proliferation

Cell proliferation was examined by bromodeoxyuridine (BrdU) incorporation at each subsequent passage according to the manufacturer protocol (Merck Millipore, Burlington, MA, USA). For this purpose adipose-derived stromal/stem cells were seeded on 96-well plates (Corning, Manassas, VA, USA) at a density of 4×10^3 cells per well. After 24-

Table 1. Antibodies Used for Analysis of the Cell Surface Marker Expression.

Antibody	Concentration (µg/ml)	Distributor
Anti-Integrin beta 1 antibody [MEM-101A] (FITC)	0.75	Abcam, UK
Anti-CD44 antibody [MEM-263] (FITC)	0.5	Abcam, UK
Anti-CD90/Thy1 antibody [5E10] (FITC)	0.5	Abcam, UK
Anti-CD11b antibody [2F4/11] (FITC)	0.5	Abcam, UK
Mouse Anti-Rat CD31 Clone [TLD-3A12] (PE)	0.5	BD Biosciences, USA
CD45 antibody [K252-1E4] (FITC)	0.5	GeneTex, USA
Mouse IgG1 kappa [MOPC-21] (FITC)	0.5	Abcam, USA
Mouse IgG1, kappa [MOPC-31C] (PE)	0.5	BD Biosciences, USA

FITC: fluorescein isothiocyanate; PE: phycoerythrin.

h culture, 20 µl of the diluted BrdU label was added to the appropriate wells. At the end of the incubation time (48 h) cell culture medium was removed and 200 µl of Fixing Solution was added to each well. Cells were fixed for 30 min at room temperature. After fixation, cells were rinsed with 1× Wash Buffer and incubated with 100 µl of prediluted anti-BrdU monoclonal antibody for 1 h at room temperature. Then cells were again washed and incubated with goat anti-mouse immunoglobulin G peroxidase conjugate for 30 min at room temperature. After the final wash, 100 µl of TMB Peroxidase Substrate was added to each well and cells were incubated for 30 min at room temperature in the dark. To stop the reaction 100 µl of acid Stop Solution was pipetted to each well. The absorbance was measured at 450 nm (Varioskan LUX, Thermo Fisher Scientific).

Viability

Cell viability was examined by MTT (3-(4,5-dimethylthiazol-2-yl)-2,5-diphenyltetrazolium bromide) assay at each subsequent passage. Adipose-derived stromal/stem cells were seeded on 96-well plates at a density of 4×10^3 cells per well. After 48 h culture, cells from each well were rinsed with PBS (Corning) and incubated with 50 µl of 1 mg/ml MTT solution (Sigma-Aldrich) for 2 h in 37°C. After the incubation, MTT solution was removed and formazan crystals were dissolved in 200 µl of dimethyl sulfoxide (POCH, Poland). The absorbance was measured at 570 nm (Varioskan LUX, Thermo Fisher Scientific).

Clonogenicity

Reproductive viability was examined by colony-forming assay every second passage. Adipose-derived stromal/stem

cells were seeded on six-well plates (Corning) at a density of 1×10^2 cells per well. After 10-d culture, cell colonies were rinsed with 2 ml of 0.9% saline (Avantor, Gliwice, Poland) and stained with 0.25% methylene blue solution (Sigma-Aldrich). Colonies containing more than 50 individual cells were counted using a stereomicroscope (Leica).

Apoptosis

DNA fragmentation was detected with the APO-DIRECT Kit (BD Biosciences) according to the manufacturer protocol. Every second passage, approximately 1×10^6 cells were fixed in 1% paraformaldehyde for 30 min. Then cells were centrifuged for 5 min at $700 \times g$, suspended in PBS, and after subsequent centrifugation fixed in 70% ethanol (Avantor). After overnight incubation at -20°C , the cells were centrifuged and suspended in 1× Wash Buffer. In the next step cells were suspended in 50 µl of DNA Staining Solution containing terminal deoxynucleotidyl transferase and FITC-dUTP (fluorescein isothiocyanate-deoxyuridine triphosphate) for 60 min at 37°C . At the end of the incubation time 1 ml of Rinse Buffer was added and cells were centrifuged. Then cells were suspended in 1 ml of Rinse Buffer and 0.5 ml of the PI/RNase Staining Buffer. After 30 min incubation in room temperature, cells were analyzed with the use of FACSCanto II flow cytometer (BD Biosciences). Results were compared to negative (live cells) and positive (apoptotic cells) controls provided by the manufacturer.

Cell Cycle

Cell cycle progression was determined with the use of Tali Cell Cycle Kit (Thermo Fisher Scientific) followed by flow cytometry analysis. Every second passage, approximately 1×10^6 cells were suspended in PBS and subsequently fixed in ice-cold 70% ethanol. Cells were kept in ethanol overnight at -20°C and then centrifuged for 5 min at $700 \times g$. The obtained cell pellet was suspended in PBS. After subsequent centrifugation cells were suspended in 200 µl of Staining Solution composed of propidium iodide, RNase A, and Triton X-100, incubated for 30 min in the dark at room temperature and analyzed with the use of FACSCanto II flow cytometer. Obtained data were analyzed using FlowJo v10 (Becton, Dickinson and Company, USA). Percentage of cells in G0/G1, S, and G2/M phases were calculated using Dean–Jett–Fox model.

Senescence-Associated β -Galactosidase Activity

β -galactosidase activity in senescent cells was measured cytochemically at pH 6 every second passage with the use of Senescence Cells Histochemical Staining Kit (Sigma-Aldrich). Adipose-derived stromal/stem cells were seeded on 35-mm tissue culture dishes at a density of 2×10^3 cells per dish. After 48 h culture, cells were rinsed with PBS and fixed for 5 min at room temperature with 1.5 ml of 1× Fixing

Buffer. Cells were then rinsed with PBS and finally 1 ml of Staining Mixture, prepared according to the manufacturer protocol, was added to each dish. Dishes were incubated overnight at 37°C without CO₂. Stained cells were counted under an inverted microscope (Leica).

Differentiation Potential—Adipogenesis

AD-MSCs differentiation into adipocytes was induced with the use of Mesenchymal Adipogenesis Kit (Merck Millipore). Adipose-derived stromal/stem cells at P2, P6, and P10 were seeded on six-well plates (Corning) at a density of 1.2×10^5 cells per well for qualitative analysis and on 96-well plates at a density of 1.2×10^4 cells per well for quantitative analysis. After 72 h culture medium was replaced with 1 ml or 200 μ l Adipogenesis Induction Medium, respectively, for 12- and 96-well plates. Medium was changed every 2 d for 21 d following differentiation schedule provided by the manufacturer. Differentiated cells were fixed with 4% formaldehyde (Sigma-Aldrich) for 30 min at room temperature, washed with PBS for 10 min, and subsequently washed with distilled water. Lipid droplets were stained with 0.37% Oil Red O Solution (Sigma-Aldrich) for 50 min at room temperature. Then cells were rinsed three times with distilled water and stained with hematoxylin solution (Sigma-Aldrich) for 10 min to visualize cell nuclei. Adipocytes containing lipid droplets were observed under an inverted microscope.

After 21-d differentiation into adipocytes, accumulation of intracellular triglycerides was determined with AdipoRed Assay Reagent (Lonza, Verviers, Belgium). After washing with PBS, 5 μ l of AdipoRed was pipetted to each well. Plates were incubated for 10 min at 37°C and then fluorescence was measured with excitation at 485 nm and emission at 572 nm (Varioskan LUX, Thermo Fisher Scientific).

Differentiation Potential—Osteogenesis

Differentiation into osteocytes was induced using StemProOsteogenesis Differentiation Kit (LifeTechnologies, Carlsbad, CA, USA). Adipose-derived stromal/stem cells at P2, P6, and P10 were seeded on six-well plates at a density of 1.8×10^4 cells per well for qualitative analysis and on 96-well plates at a density of 2×10^3 cells per well for quantitative analysis. After 72-h culture, medium was replaced with 1 ml or 200 μ l prewarmed Complete Osteogenesis Differentiation Medium, respectively, for 12- and 96-well plates. Medium was changed every 3 d for 21 d following differentiation schedule provided by the manufacturer.

After 21 d of differentiation extracellular calcium deposits were specifically stained bright orange-red using Alizarin Red S. Before staining, cells were fixed with 4% formaldehyde for 30 min at room temperature and rinsed twice with distilled water. Cells were then stained with 2% Alizarin Red S Solution (Sigma-Aldrich) for 2 min at pH 4.2. After

subsequent washing with water, calcium deposits were visualized under inverted microscope.

Differentiation hydroxyapatite portion of the bone-like nodules deposited by cells was quantitated with the use of OsteoImage Assay (Lonza). Differentiated cells were rinsed with PBS and fixed with 4% formaldehyde for 30 min at room temperature. After fixation, cells were washed twice with 1 \times Wash Buffer and then incubated with 100 μ l of Staining Reagent at room temperature, protected from the light, for 30 min. Cells were then rinsed twice with Wash Buffer. After final wash 200 μ l of diluted wash buffer was added to all wells and fluorescence was measured with excitation at 492 nm and emission at 520 nm (Varioskan LUX, Thermo Fisher Scientific).

Differentiation Potential—Chondrogenesis

Chondrogenic differentiation of adipose-derived stromal/stem cells was induced with the use of StemProChondrogenesis Differentiation Kit (LifeTechnologies). Adipose-derived stromal/stem cells at P2, P6, and P10 were seeded on 12-well plate in 5 μ l droplets containing 8×10^4 cells to generate micromass cultures. After 2-h incubation 1 ml of Chondrogenesis Induction Medium was added and cultures were reseeded every 3 d following differentiation schedule provided by the manufacturer.

After 14 d of differentiation into chondrocytes, cells were fixed with 4% formaldehyde for 30 min at room temperature and washed twice with PBS. For proteoglycans visualization micromass cultures were then stained with 1% Alcian Blue (Sigma-Aldrich) for 30 min. After subsequent washing with 0.1 N HCl and in distilled water, chondrogenic pellets were visualized under inverted microscope.

Molecular Markers of Senescence

AD-MSCs from the P2, P6, and P10 were placed in RNA-later solution (Thermo Fisher Scientific) and stored at -80°C . RNA was isolated using RNeasy Mini Kit (Qiagen, Hilden, Germany) according to the manufacturer's protocol. Quality and quantity of RNA were evaluated using NanoDrop (Thermo Fisher Scientific) and Agilent 2100 BioAnalyzer (Agilent Technologies, Santa Clara, CA, USA). Complementary DNA was synthesized from 500 ng of total RNA using RT² First Strand Kit (Qiagen). Gene expression of senesced cells was determined by real-time quantitative reverse transcriptase polymerase chain reaction according to RT² Profiler PCR Array Handbook using RT² Profiler PCR Array Pig Aging (Qiagen) on LightCycler 480 (Roche, Basel, Switzerland) (supplemental Table S1). The data analysis was performed at GeneGlobe Data Analysis.

Statistical Analysis

Each experiment was performed at least in triplicate. Average cell viability was expressed as a percentage relative to

Table 2. Immunophenotypic characterization of adipose-derived mesenchymal stromal/stem cells (AD-MSCs) in subsequent passages.

Passage	Positive surface markers (%)			Negative surface markers (%)		
	CD29	CD44	CD90	CD11b	CD31	CD45
P2	36.57 ± 8.52	85.67 ± 10.75	89.69 ± 9.17	0.18 ± 0.20	10.91 ± 8.74	0.35 ± 0.48
P4	57.53 ± 7.80	87.15 ± 9.42	88.18 ± 9.15	0.10 ± 0.00	8.01 ± 2.53	0.38 ± 0.33
P6	21.70 ± 14.12	87.12 ± 15.45	81.03 ± 12.12	0.10 ± 0.00	12.35 ± 7.95	0.28 ± 0.28
P8	24.53 ± 13.40	89.27 ± 11.64	74.98 ± 10.02	0.10 ± 0.00	12.09 ± 7.85	0.53 ± 0.60
P10	49.63 ± 11.41	85.80 ± 11.92	83.18 ± 8.19	0.10 ± 0.00	6.48 ± 2.97	0.33 ± 0.41

Values presented as a mean ± standard deviation from three independent measurements.

the control. All data were presented as means ± standard deviation. Statistical analysis was performed with Student's *t*-test using SPSS Statistica (Predictive Solutions, Cracow, Poland). The values were compared to the data from the second passage (to the first passage in the case of cell number and PDT analysis), which served as a control. Values of *P* lower than 0.05 were considered as statistically significant.

Results

Immunophenotype Analysis

Cultured AD-MSCs maintained stable expression of CD44⁺ (87.00% ± 2.24), CD90⁺ (83.41 ± 1.49), CD11b⁻ (0.12% ± 0.09), and CD45⁻ (0.38% ± 0.13) in subsequent passages (Table 2). Relatively low expression of CD29⁺ ranging between 57.5% ± 7.8% at P4 and 21.7% ± 14.1% at P6 was observed. Expression of endothelial cell marker CD31 during long-term culture was slightly increased, between 12.35% ± 7.95% at P6 and 6.48% ± 2.97% at P10 (Table 2).

Analysis of Growth Kinetics and Morphology of AD-MSCs

To examine the long-term growth kinetics, the cell number in subsequent passages, starting with the first passage of AD-MSC primary culture, was determined. The highest average number of AD-MSCs obtained at P1 and P2, respectively, was 15.7 × 10⁶ and 16.0 × 10⁶ cells. After P2 we observed a gradual decrease in cell number (Fig. 1A). The decrease in the number of cells was accompanied by an increase in the PDT (Fig. 1B). Average PDT between P2 and P12 increased 2.8-fold. Statistically significant decrease in PDT was observed at P7 and subsequent passages (Fig. 1B).

During the long-term AD-MSC culture we observed morphological changes typical for senescent cells. At early passages AD-MSCs were morphologically a homogenous population of small and spindle-shaped cells (Fig. 2A). Between P6 and P8 the cells became much larger and got irregular shape (Fig. 2F). The appearance of dark inclusions in cytoplasm was observed from P6 (Fig. 2C).

Analysis of AD-MSC Proliferation

Relative levels of BrdU incorporated into DNA during the S phase of the cell cycle gradually decreased at subsequent passages (Fig. 1C). The highest proliferation index was observed at P2. Between P2 and P3, BrdU incorporation decreased significantly by 29.6% (*P* < 0.05). At late passages (>P10) BrdU incorporation remained relatively constant.

Viability Analysis

The differences in cell viability between P2 and P8, as measured spectrophotometrically, were not statistically significant (values between 0.68 ± 0.10 and 0.55 ± 0.08, *P* > 0.05). The highest decrease in cell viability was observed between P9 and P10, approximately 34.2%. Similar to BrdU incorporation, mitochondrial dehydrogenase activity remained constant in late passages (>P10) (Fig. 1D).

Clonogenicity Analysis

The colony-forming potential of AD-MSCs decreased with subsequent passages. Clonogenic efficiency between P2 and P6 ranged between 75.2 and 63.2 per 1 × 10³ cells plated. Statistically significant reduction in the AD-MSCs clonogenicity by 54.4% appeared at P8 (*P* < 0.05). Clonogenic potential at P10 and P12 decreased, respectively, to 23.5 and 20.6 per 1 × 10³ cells plated (Fig. 1E).

DNA Fragmentation Analysis

Activation of endonucleases during the apoptotic program was analyzed on the basis of DNA breaks labeling with FITC-dUTP, followed by flow cytometric analysis. No differences in fluorescence intensities at subsequent passages after staining cells with FITC-labeled anti-BrdU antibody were observed (Fig. 3C). Average fluorescence intensities of DNA breaks in AD-MSCs between P2 and P10 ranged between 0.13% and 0.55% ± 0.24% and were similar to negative control cells (0.86% ± 0.21%) (*P* > 0.05).

Cell Cycle Analysis

Analysis showed lack of changes in cell distribution between each cell cycle phase in long-term culture (Fig. 3A, B).

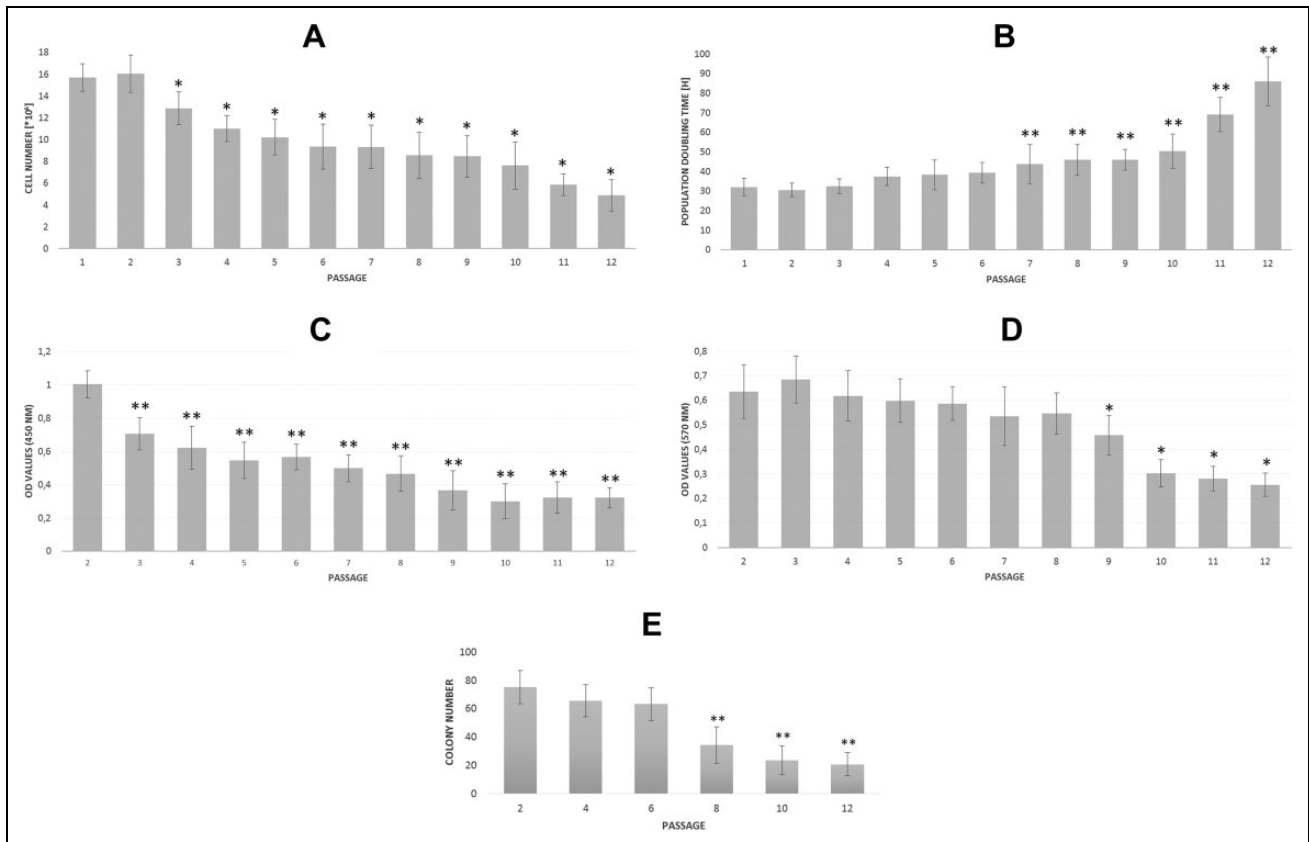


Fig. 1. Properties of AD-MSCs during long-term in vitro culture. (A) Average number of AD-MSCs at subsequent passages. (B) Average population doubling time of AD-MSCs at subsequent passages. (C) Cell proliferation assessed on the basis of bromodeoxyuridine incorporation into newly synthesized DNA strands. (D) Cell viability measured with the use of 3-(4,5-dimethylthiazol-2-yl)-2,5-diphenyltetrazolium bromide assay. (E) Clonogenic potential of AD-MSCs in subsequent passages. Bars represent standard deviation. Statistically significant differences: * $P < 0.05$, ** $P < 0.001$.

AD-MSC: adipose-derived mesenchymal stromal/stem cell; OD: optical density.

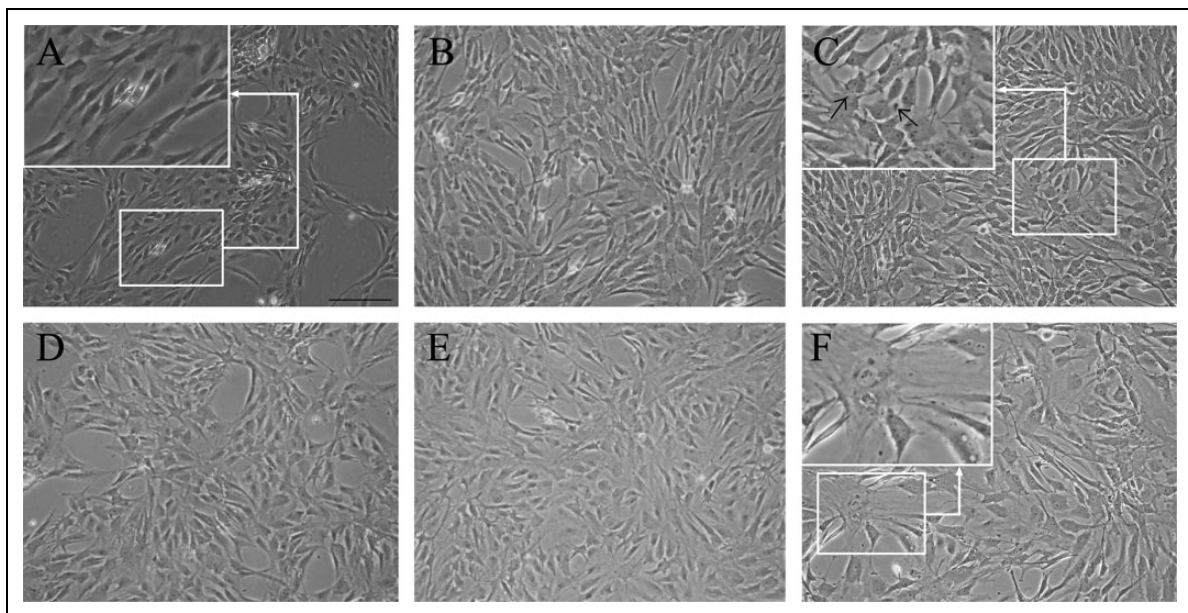


Fig. 2. Morphology of adipose-derived mesenchymal stromal/stem cells during a long-term in vitro culture. Passages: P2(A), P4(B), P6(C), P8(D), P10(E), P12(F). Small and spindle-shaped cells (A); appearance of dark inclusions (C, arrow); cells become much larger and get irregular shape (F). Images were taken on the Nikon phase-contrast microscope (objective magnification 10 \times).

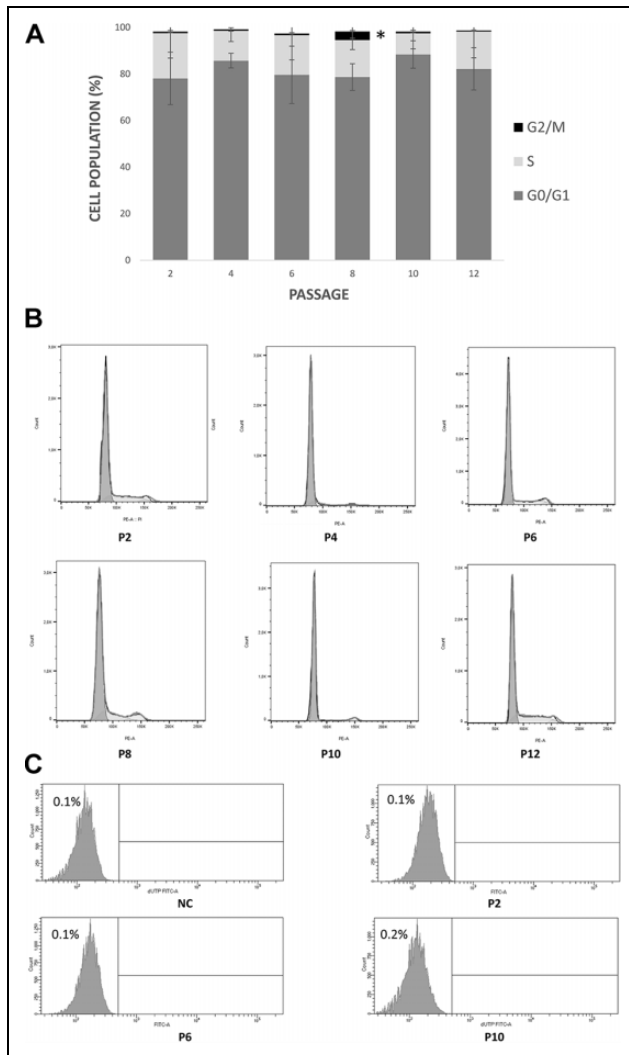


Fig. 3. Cell cycle and apoptosis profiles of adipose-derived stromal cells during long-term culture. (A) Percentages of cells in G0/G1, S, and G2/M phases of the cell cycle. (B) Representative FACS histograms of AD-MSC DNA content. (C) Representative FACS histograms for analyzed DNA breaks in AD-MSCs at P2, P6, P10, and NC. Statistically significant differences: * $P < 0.05$.

AD-MSC: adipose-derived mesenchymal stromal/stem cell; FACS: fluorescence-activated cell sorting; NC: negative control.

Differences were observed only in P8 in which more cells cumulate in G2/M phase, and this effect was not observed in other passages.

Analysis of AD-MSCs' Differentiation Potential

Adipogenic differentiation confirmed by lipid vesicles formation was the most effective at P2 (Fig. 4A). At P6 and P10 accumulation of intracellular triglycerides in differentiated cells was similar to undifferentiated control.

Surprisingly, the most effective osteogenic differentiation was noted at P6, when 4.65-fold increase in hydroxyapatite portion of bone-like nodules deposited by cells was observed (Fig. 4A, B). Chondrogenic differentiation was confirmed on the basis of Alcian Blue staining. Despite the same initial cell number used for micromass culture generation, cell pellets from P2 were larger and denser than those from P6 and P10 (Fig. 4A). The Alcian Blue staining intensity decreased with subsequent passages.

β -Galactosidase Activity Analysis

At early passages (<P8) only single cells were positive for senescence-associated β -galactosidase activity (SA- β -gal). A gradual and significant increase of β -galactosidase-positive senescence cells was observed from P8 to P12 ($P < 0.05$). The number of AD-MSCs positive for SA- β -gal increased from 70.0 at P8 to 153.3 at P12 (Fig. 5).

Molecular Analysis of Senescence-Related Genes

Molecular analysis revealed a different senescence gene expression profile in subsequent AD-MSC passages (Fig. 6, Table 3). After P6 compared to P2 we observed overexpression of 18 genes and underexpression of 11 genes. After P10, the number of overexpressed genes increased up to 29 and underexpressed to 13 (Fig. 6A, B). The hierarchical clustering performed for all analyzed passages divided differentially expressed genes (DEGs) into two main clusters: AD-MSCs from P2 together with P6 and AD-MSCs from P10. The gene expression profile in cells at P2 was comparable to the profile observed in cells at P6. This differed from the gene expression profile observed in AD-MSCs at P10 (Fig. 6C). Analysis of DEGs using the STRING database version 11.0 allows for detection of four pathways, which could play potential role in AD-MSCs aging⁹. The largest number of genes (eight) was involved in complement and coagulation cascade (C3, C4, C1QA, C1QC, CFH, CLU, C3AR1, C5AR1), six genes were involved in phagosome activation (C3, CTSS, CD14, TLR2, TLR4, and FCGR1A), four genes in Toll-like receptor signaling pathway (CD14, TLR2, TLR4, and SPP1), and three genes in NOD-like receptor signaling pathway (TLR4, CASP1, and TXNIP). Analysis of these genes using STRING and KEGG PATHWAY databases detected interactions between all four pathways. As a result of this analysis we concluded that senescence of AD-MSCs was related to alteration of genes' expression involved in activation of inflammatory process leading to growth inhibition and cell death through phagocytosis (Fig. 7).

Discussion

In this study we analyzed the biological properties of porcine AD-MSCs in a long term in vitro culture (12 passages) focusing on molecular aspects of cellular senescence. We

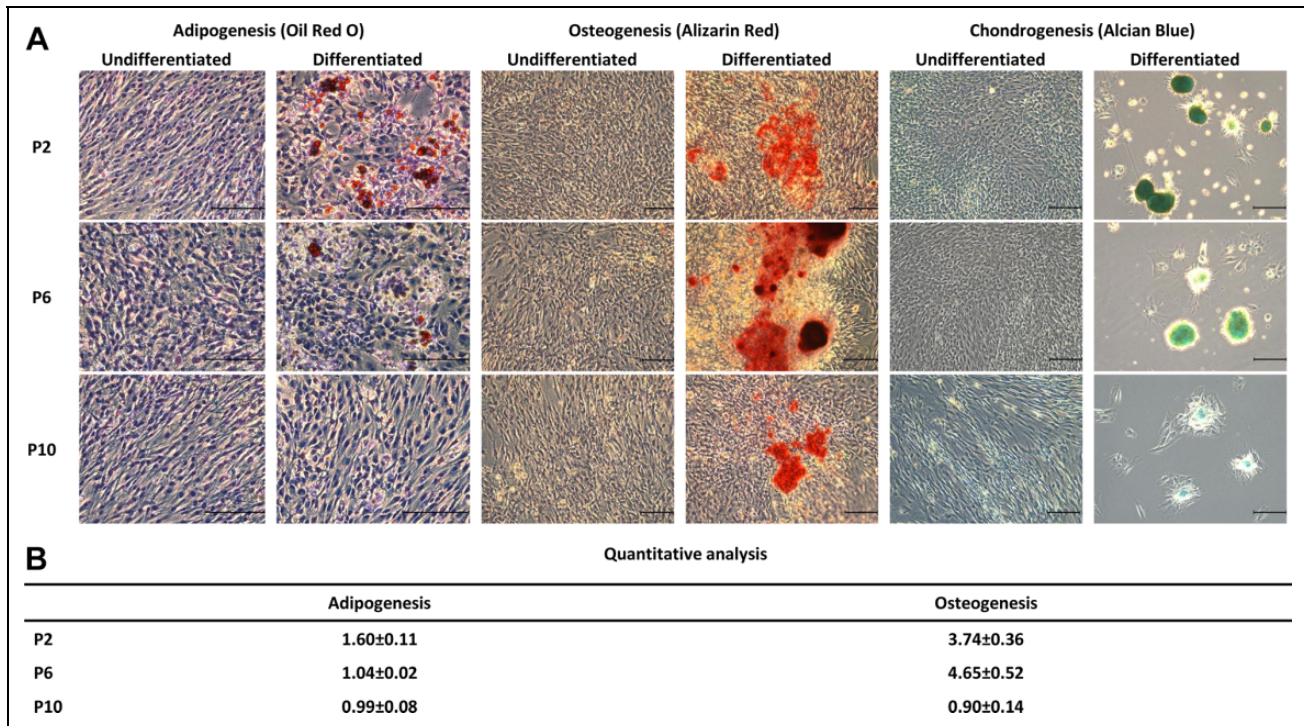


Fig. 4. Differentiation potential of adipose-derived mesenchymal stromal/stem cells during long-term culture. (A) Experiment assessed on the basis of qualitative analysis of lipid vesicles formation (adipogenesis using Oil Red O staining), presence of mineralized nodules (osteogenesis using Alizarin Red staining) and proteoglycans synthesis (chondrogenesis using Alcian Blue staining). (B) Experiment using quantitative analysis using AdipoRed Assay Reagent (Lonza) for adipogenesis and OsteoImage Assay (Lonza) for osteogenesis. Results obtained in P6 and P10 were statistically significant compared to P2 ($P < 0.01$).

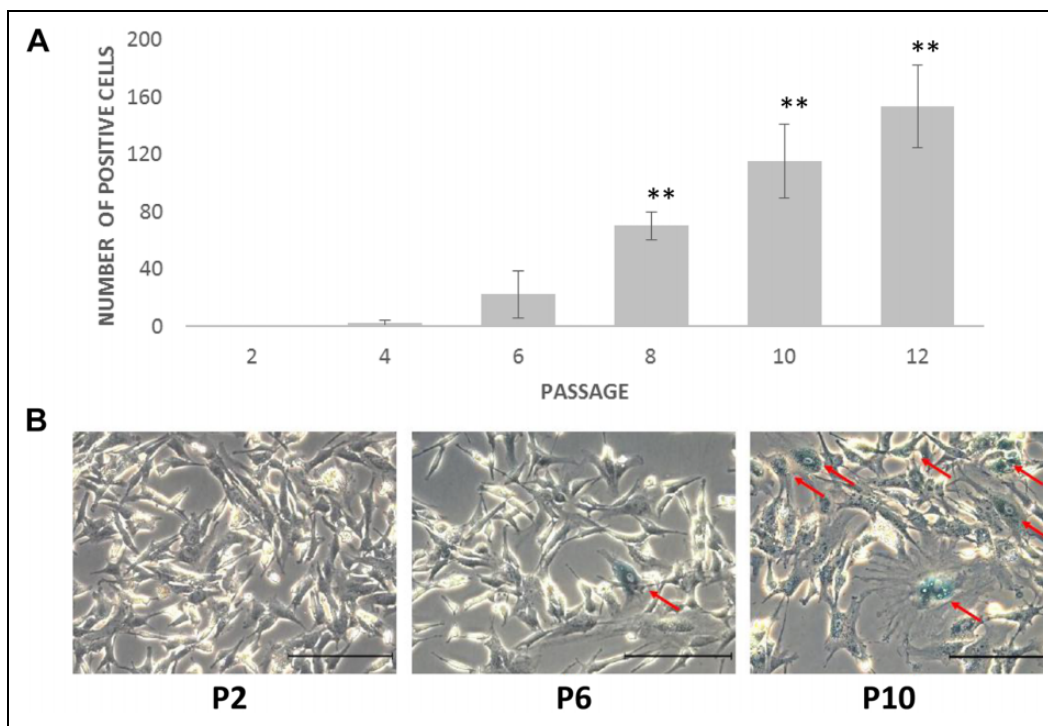


Fig. 5. β -galactosidase expression in long-term AD-MSC culture. (A) Number of SA- β -gal-positive AD-MSCs at different passages. (B) AD-MSCs stained for SA- β -gal. Arrows indicate senescent cells. Scale bar, 200 μ m. Statistically significant differences: ** $P < 0.001$. AD-MSC: adipose-derived mesenchymal stromal/stem cell.

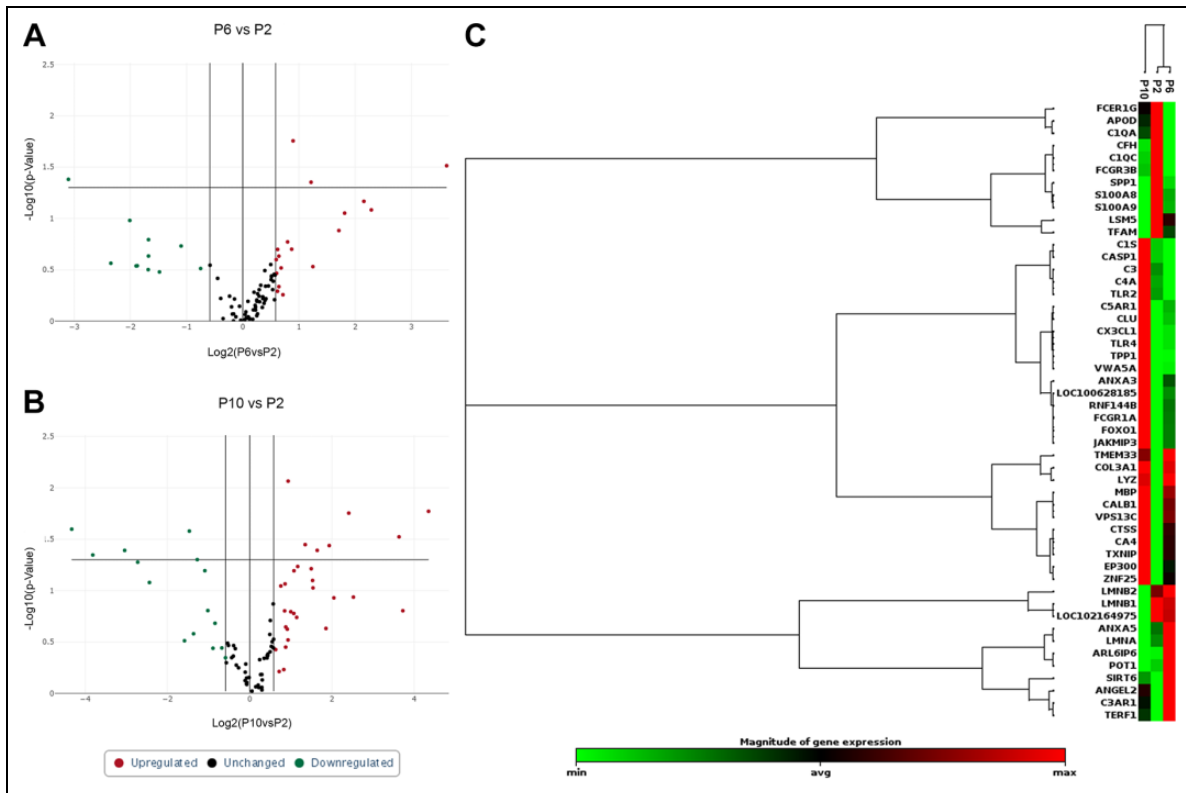


Fig. 6. Changes in senescence-related gene expression in adipose-derived mesenchymal stromal/stem cell culture. (A, B) Results from RT² Profiler PCR Arrays Pig Aging plate. (C) Hierarchical clustering of differentially expressed genes.

cultured AD-MSCs till P12 because after that time (about 40 d of culture) they changed significantly their morphology and decreased proliferation rate what in consequence leads to getting even smaller cell numbers than initially seeded. Obtained results showed that during the first eight passages most of the AD-MSC properties were on the same comparable to P2 level. Only significant decrease in cell number and BrdU incorporation after P3 and P2, respectively, was observed (Fig. 1A, C). After P8 we observed about 50% reduction in cell number compared to P2 what can be a potential problem in obtaining a suitable cell number for cell therapies or construction of neo-tissues or neo-organs using tissue engineering approach. Doubling times ranged between 30 and 50 h till P10 and increased up to 90 h at P12, which is consistent with another work in which dental pulp and bone marrow mesenchymal stem cells were analyzed¹⁰. In another study conducted on human and rhesus bone marrow mesenchymal stem cells (BM-MSCs) and AD-MSCs, doubling time reach 120 h at the end of culture (P20–P30)¹¹. Mesenchymal stromal cells isolated from human chorionic villi kept the doubling time value on the level of 30 h till P10, reaching about 60 h at P20¹². Another study performed on BM-MSCs together with umbilical cord mesenchymal stem cells (UC-MSCs) also showed decreasing proliferation capacity with prolonged culture time (P12)¹³.

Morphological changes typical for senescent cells were observed after the P6 (about 21 d). Similar findings were noticed for BM-MSCs. After 84 d of culture intracellular granules were observed. Longer culture resulted in cell vacuolization and cell fragmentation visualized as debris in culture medium¹⁴. In another study performed on human AD-MSCs the first morphological changes appeared after the P7, with the cells becoming larger with wider cytoplasmic projections¹⁵. Higher passages (P20–P30) resulted in irregular morphology with more granular cytoplasm and increasing number of cellular debris in culture medium. During subsequent passages shortening of telomeres was observed. In our study cell senescence was analyzed by measuring β -galactosidase activity and analysis of senescence-related gene expression. Increasing expression of β -galactosidase appears in aging cells, which is a consequence of morphological changes with the increase in the abundance of lysosomal enzyme, which could be linked with increased lysosomal biogenesis observed in senescent cells¹⁶. In our study, level of β -galactosidase activity increased gradually with subsequent passages (Fig. 5), which was compatible with changes in cell morphology (Fig. 2). Similar results were observed in hair follicle mesenchymal stem cells (HF-MSCs) in which aging cells in greater number started to appear after P8 (in our study after P6)¹⁷. In the case of human and rhesus BM-MSCs and AD-MSCs

Table 3. Differential Senescence-Related Gene Expression in Subsequent Passages.

Expression	P6 vs. P2	P10 vs. P2	
Upregulated	ANGEL2	ANGEL2	
	ANXA5	ANXA3	
	ARL6IP6	C1S	
	C3AR1	C3	
	CA4	C3AR1	
	CALB1	C4A	
	CD14	C5AR1	
	COL3A1	CA4	
	CTSS	CALB1	
	CX3CL1	CASPI	
	LMNA	CLU	
	LYZ	COL3A1	
	MBP	CTSS	
	POT1	CX3CL1	
	SIRT6	EP300	
	TERFI	FCGR1A	
	TMEM33	FOXO1	
	TXNIP	JAKMIP3	
		LOC100628185	
		LYZ	
		MBP	
		RNF144B	
		TLR2	
		TLR4	
		TPPI	
		TXNIP	
		VPS13C	
		VWA5A	
		ZNF25	
	Downregulated	APOD	APOD
		CIQA	CIQC
		CIQC	CFH
		C3	FCER1G
		C4A	FCGR3B
		CFH	LMNB1
		FCER1G	LMNB2
FCGR3B		LOC102164975	
S100A8		LSM5	
S100A9		S100A8	
SPPI		S100A9	
		SPPI	
	TFAM		

significant increase in the number of aging cells (76% and 95%, respectively) appeared after P20, compared to P12 in our study¹¹.

Another symptom indicating cell senescence is loss of differentiation potential. We observed decrease of adipogenic and chondrogenic potential after P6 and osteogenic potential after P10. In the study of Bonab et al., decrease of BM-MSCs' osteogenic potential after P8 and adipogenic after P6 was observed¹⁴. Similar observation was done in the case of HF-MSCs, and difference was noticed only in the case of osteogenic potential, which increased after P8 compared to P5 but significantly decreased after P11¹⁷. Human and rhesus BM-MSCs and AD-MSCs retained their

multipotential capacity at least up to P10¹¹. Study conducted on omentum AD-MSCs showed that even long-term culture (P20) did not affect osteogenic and adipogenic potential¹⁸. In another study even after P15 no differences in adipogenic, chondrogenic, and osteogenic potential of tonsil MSCs was observed, and long-term culture effected in decrease of proliferative potential measured by colony-forming unit and MTT assay. Colony-forming unit decreased about 35% at P15 passage (in our study about 54% after P8)¹⁹.

Changes in cell cycle profile were observed in dental pulp, peripheral blood, and umbilical cord blood MSCs. Additionally, in the case of peripheral blood mesenchymal stem cells (PB-MSCs) and UC-MSCs increase in apoptotic cell number was noticed^{10,20,21}. Increase in apoptotic cell number appeared after P20 in the case of UC-MSCs²¹. In our study no changes in cell distribution in cell cycle phases and in number of apoptotic cells were observed throughout the study period (Fig. 3C).

Mesenchymal stromal/stem cells are characterized by expression of specific surface markers like CD90, CD44, or CD29 and lack of antigen expression like CD11b, CD31, and CD45 (Fig. 6). Our results showed that expression of most studied markers was stable in long-term culture, which is consistent with the results of Marappagounder et al. who also noticed maintenance of characteristic AD-MSC markers in prolonged culture¹⁸. Another study conducted on human AD-MSCs also confirmed stability of their phenotype in long culture, even after P30¹⁴. Similar results were also observed in the case of BM-MSCs and UC-MSCs¹³. In our study instability of two antigens, CD29 and CD31, was observed. According to the recommendation of the International Society for Cell & Gene Therapy both CD29 and CD31 are not considered in minimal criteria to define multipotent MSCs; however, in literature these two antigens were examined for identification of AD-MSCs²². Expression of surface markers can vary between MSCs obtained from different sources, for example in the case of AD-MSCs positive expression of CD34 can be detected while in general this is a negative marker in other types of MSCs. According to this information positive expression of CD31 antigen in the case of AD-MSCs is also possible. Criteria for MSC identification were established for human cells. We have performed experiment on porcine cells, which probably could affect final results.

From our knowledge this is the first study in which porcine AD-MSCs were analyzed for senescence genes expression using RT² Profiler PCR Array. Molecular analysis showed a different expression pattern of genes involved in senescence. After P6 compared to P2 we observed overexpression of 18 genes and underexpression of 11 genes. After P10 the number of overexpressed genes increased up to 29 and underexpressed to 13. Analysis of differentially expressed genes using the STRING database version 11.0 allows for identification of four pathways which could play a potential role in AD-MSCs aging: complement and

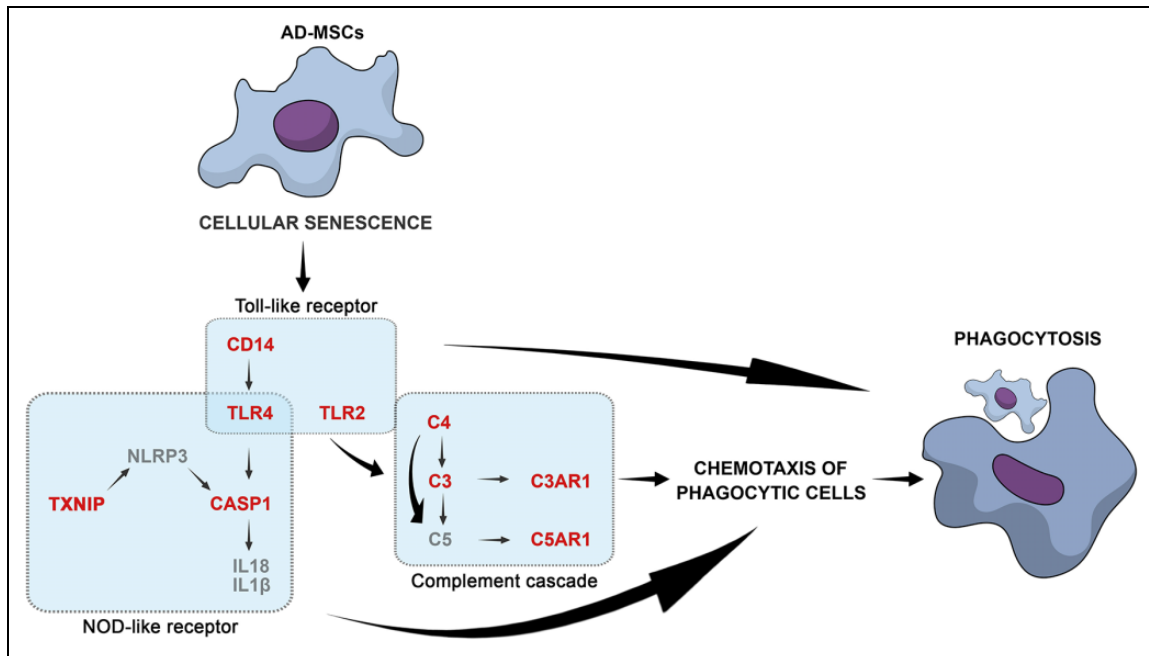


Fig. 7. Potential pathway leading to phagocytosis of senescent AD-MSCs. Molecular analysis showed that during a long-term culture of AD-MSCs activation of genes involved in immune response was observed, which in consequence leads to phagocytosis of senescent cells. Overexpressed genes are marked in red.

AD-MSC: adipose-derived mesenchymal stromal/stem cell.

coagulation cascade, phagosome, Toll-like receptor signaling pathway, and NOD-like receptor signaling pathway⁹. These pathways are activated mainly as a result of immunological response. Senescent cells are regarded as proinflammatory and immunogenic, playing active roles both in activation and recruitment of the immune system. Additionally senescent cells may persist indefinitely within tissue until their removal by the immune system, necrosis, or other forms of cell death²³. All four pathways detected in this study are directly connected to each other. A pathway that connects all pathways together seems to be the Toll-like receptor signaling pathway. In our study we observed overexpression of four genes involved in this pathway (TLR2, TLR4, CD14, and SPP1) from which TLR4 seems to play a key role. This protein is also involved in NOD-like signaling receptor pathway leading to activation of caspase 1, which is additionally activated by NLRP3 (activated also by TXNIP overexpressed in our study). Activation of Caspase-1 induces maturation and releases proinflammatory cytokines (IL18 and IL1β). Creation of NLRP3 inflammasome is closely related to cellular senescence and was observed in endothelial cells, cardiac fibroblasts, and primary BM-MSCs^{24,25}. Toll-like signaling pathway is involved in activation of complement and coagulation cascade; in our study, five genes, involved in the complement cascade pathway, were overexpressed after P12 (C3, C4A, CLU, C3AR1, and C5AR1). C3 protein leads to activation of CR1 and CR3 genes, which consequently induce phagocytosis, and this process is also activated by overexpression of Toll-like

receptor signaling pathway (CD14, TLR2, and TLR4). Activation of C3AR1 and C5AR1 generates chemotaxis of phagocytic cells to the place of ongoing inflammatory process, which helps in one complement cascade function: elimination of modified or damaged host cells²⁶. Taking together, the probable mechanism of AD-MSC senescence on the basis of molecular analysis of cells after P10 is activation of immune response and phagocytosis of senescent cells (Fig. 7). Activation of immune system by senescence cells was also described by Burton and Stolzing, and cells like macrophages have the potential to cell death induction in these cells by phagocytosis²⁷. Similar mechanism of MSCs senescence was described by Shi et al., and in their study TLR4 activation was induced by S100A9²⁴. In our study both S100A9 and S100A8 were underexpressed, which indicate that expression of these proteins is not required for activation of proposed AD-MSCs' senescence mechanism.

MSCs changed their properties (differentiation potential, growth dynamics, and cell morphology) in in vitro culture during subsequent passages^{28,29}. According to the obtained results, this effect is not related with donor because tissues for cell isolations were collected from animals at the same age. Observed cellular senescence can be related to medium effect. Growth conditions and metabolic needs differ significantly in in vitro culture. Culture medium contains less number of growth factors and other supplements like amino acids than are normally found in extracellular tissue fluid. Additionally after isolation and during the culture cells continuously undergo proliferation, which generate unnatural stress to

cells^{30,31}. Our results showed that the best time point up to which AD-MSCs should be used for further in vitro and in vivo experiments is the P6, until which most of the AD-MSC properties were maintained comparable to early P2 level. However, after that time 50% reduction of cell number compared to first culture days was observed, which can be a potential problem in obtaining a suitable cell number for construction of neo-tissues or neo-organs. The balance between proper cell number and maximum passage number necessary to obtain suitable cell amount should be preserved.

Ethical Approval

Ethical approval to report this case was obtained from the Local Ethics Committee in Bydgoszcz, Poland (no. 30/2013).

Statement of Human and Animal Rights

All procedures in this study were conducted in accordance with the Local Ethics Committee in Bydgoszcz, Poland (no. 30/2013) approved protocols.

Statement of Informed Consent

There are no human subjects in this article and informed consent is not applicable.


Declaration of Conflicting Interests

The author(s) declared no potential conflicts of interest with respect to the research, authorship, and/or publication of this article.

Funding

The author(s) disclosed receipt of the following financial support for the research, authorship, and/or publication of this article: The present work was supported by the National Center for Research and Development (NCBR) in Poland under Agreement no. STRATEGMED1/235368/8/NCBR/2014 (Smart AUCI Project) within the Strategic Programme STRATEGMED "Prevention practices and treatment of civilization diseases."

ORCID iD

Tomasz Kloskowski  <https://orcid.org/0000-0001-5599-9315>

Supplemental Material

Supplemental material for this article is available online.

References

- Zuk P. Adipose-derived stem cells in tissue regeneration: a review. *IRS Stem Cell*. 2013;2013:713959.
- Kloskowski T, Kowalczyk T, Nowacki M, Drewa T. Tissue engineering and ureter regeneration: is it possible? *Int J Artif Organs*. 2013;36(6):392–405.
- De Francesco F, Ricci G, D'Andrea F, Nicoletti GF, Ferraro GA. Human adipose stem cells: from bench to bedside. *Tissue Eng Part B Rev*. 2015;21(6):572–584.
- Minteer D, Marra KG, Rubin JP. Adipose-derived mesenchymal stem cells: biology and potential applications. *Adv Biochem Eng Biotechnol*. 2013;129:59–71.
- Minteer DM, Marra KG, Rubin JP. Adipose stem cells: biology, safety, regulation, and regenerative potential. *Clin Plast Surg*. 2015;42(2):169–179.
- Włodarski KH, Włodarski P, Galus R, Mazur S. Adipose mesenchymal stem cells. Their characteristics and potential application in tissue repair. *Pol Orthop Traumatol*. 2012;77:97–99.
- Atala A, Bauer SB, Soker S, Yoo JJ, Retik AB. Tissue-engineered autologous bladders for patients needing cystoplasty. *Lancet*. 2006;367(9518):1241–1246.
- Pokrywczynska M, Jundzill A, Warda K, Buchholz L, Rasmus M, Adamowicz J, Bodnar M, Marszalek A, Helmin-Basa A, Michalkiewicz J, Gagat M, et al. Does mesenchymal stem cell source influence smooth muscle regeneration in tissue engineered urinary bladder? *Cell Transplant*. 2017;26(11):1780–1791.
- Szklarczyk D, Gable AL, Lyon D, Junge A, Wyder S, Huerta-Cepas J, Simonovic M, Doncheva NT, Morris JH, Bork P, Jensen LJ, et al. STRING v11: protein-protein association networks with increased coverage, supporting functional discovery in genome-wide experimental datasets. *Nucleic Acids Res*. 2019;47(D1):D607–D613.
- Suchánek J, Soukup T, Ivancaková R, Karbanová J, Hubková V, Pytlík R, Kucerová L. Human dental pulp stem cells—isolation and long term cultivation. *Acta Medica (Hradec Kralove)*. 2007;50(3):195–201.
- Izadpanah R, Kaushal D, Kriedt C, Tsien F, Patel B, Dufour J, Bunnell BA. Long-term in vitro expansion alters the biology of adult mesenchymal stem cells. *Cancer Res*. 2008;68(11):4229–4238.
- Roselli EA, Lazzati S, Iseppon F, Manganini M, Marcato L, Gariboldi MB, Maggi F, Grati FR, Simoni G. Fetal mesenchymal stromal cells from cryopreserved human chorionic villi: cytogenetic and molecular analysis of genome stability in long-term cultures. *Cytotherapy*. 2013;15(11):1340–1351.
- de Witte SFH, Lambert EE, Merino A, Strini T, Douben HJCW, O'Flynn L, Elliman SJ, de Klein AJEMM, Newsome PN, Baan CC, Hoogduijn MJ. Aging of bone marrow- and umbilical cord-derived mesenchymal stromal cells during expansion. *Cytotherapy*. 2017;19(7):798–807.
- Bonab MM, Alimoghaddam K, Talebian F, Ghaffari SH, Ghavamzadeh A, Nikbin B. Aging of mesenchymal stem cell in vitro. *BMC Cell Biol*. 2006;7:14.
- Danisovic L, Oravcova L, Krajciová L, Varchulova Novakova Z, Bohac M, Varga I, Vojtassak J. Effect of long-term culture on the biological and morphological characteristics of human adipose tissue-derived stem cells. *J Physiol Pharmacol*. 2017;68(1):149–158.
- Debacq-Chainiaus F, Erusalimsky JD, Campisi J, Toussaint O. Protocols to detect senescence-associated beta-galactosidase (SA-beta-gal) activity, a biomarker of senescent cells in culture in vivo. *Nat Protoc*. 2009;4(12):1798–1806.
- Bajpai VK, Mistriotis P, Andreadis ST. Clonal multipotency and effect of long-term in vitro expansion on differentiation potential of human hair follicle derived mesenchymal stem cells. *Stem Cell Res*. 2012;8(1):74–84.

18. Marappagounder D, Somasundaram I, Janvikula RS, Dorairaj S. Long-term culture optimization of human omentum fat-derived mesenchymal stem cells. *Cell Biol Int*. 2012;36(11):1029–1036.
19. Choi JS, Lee BJ, Park HY, Song JS, Shin SC, Lee JC, Wang SG, Jung JS. Effects of donor age, long-term passage culture, and cryopreservation on tonsil-derived mesenchymal stem cells. *Cell Physiol Biochem*. 2015;36(1):85–99.
20. Fu WL, Li J, Chen G, Li Q, Tang X, Zhang CH. Mesenchymal stem cells derived from peripheral blood retain their pluripotency, but undergo senescence during long-term culture. *Tissue Eng Part C Methods*. 2015;21(10):1088–1097.
21. Chen G, Yue A, Ruan Z, Yin Y, Wang R, Ren Y, Zhu L. Monitoring the biology stability of human umbilical cord-derived mesenchymal stem cells during long-term culture in serum-free medium. *Cell Tissue Bank*. 2014;15(4):513–521.
22. Viswanathan S, Shi Y, Galipeau J, Krampera M, Leblanc K, Martin I, Phinney DG, Sensebe L. Mesenchymal stem versus stromal cells: International Society for Cell & Gene Therapy (ISCT) mesenchymal stromal cell committee position statement on nomenclature. *Cytherapy*. 2019;21(10):1019–1024.
23. Soto-Gamez A, Quax WJ, Demaria M. Regulation of survival networks in senescent cells: From mechanisms to interventions. *J Mol Biol*. 2019;431(15):2629–2643.
24. Shi L, Zhao Y, Fe C, Gou J, Jia Y, Wu D, Wu L, Chang C. Cellular senescence induced by S100A9 in mesenchymal stromal cells through NLRP3 inflammasome activation. *Aging*. 2019;11(21):9629–9642.
25. Latz E, Xiao TS, Stutz A. Activation and regulation of the inflammasomes. *Nat Rev Immunol*. 2013;13(6):397–411.
26. West EE, Kolev M, Kemper C. Complement and the regulation of T cell responses. *Annu Rev Immunol*. 2018;36:309–338.
27. Burton DGA, Stolzing A. Cellular senescence: immunosurveillance and future immunotherapy. *Ageing Res Rev*. 2018;43:17–25.
28. Turinetto V, Vitale E, Giachino C. Senescence in human mesenchymal stem cells: Functional changes and implications in stemcell-based therapy. *Int J Mol Sci*. 2016;17(7):1164.
29. Raggi C, Berardi AC. Mesenchymal stem cells, aging and regenerative medicine. *Muscles Ligaments Tendons J*. 2012;2(3):239–242.
30. Chen H, Li Y, Tollefsbol TO. Cell senescence culturing methods. *Methods Mol Biol*. 2013;1048:1–10. doi: 10.1007/978-1-62703-556-9_1.
31. Phipps SMO, Berletch JB, Andrews LG, Tollefsbol TO. Aging cell culture. Methods and observations. *Methods Mol Biol*. 2007;371:9–19.